Binder-free Ge-three dimensional graphene electrodes for high-rate capacity Li-ion batteries

Wang, C. D.; Chui, Y. S.; Li, Y.; Chen, X. F.; Zhang, W. J.

Published in:
Applied Physics Letters

Published: 16/12/2013

Document Version:
Final Published version, also known as Publisher's PDF, Publisher's Final version or Version of Record

Published version (DOI):
10.1063/1.4851955

Publication details:
Wang, C. D., Chui, Y. S., Li, Y., Chen, X. F., & Zhang, W. J. (2013). Binder-free Ge-three dimensional graphene electrodes for high-rate capacity Li-ion batteries. *Applied Physics Letters*, *103*(25), Article 253903. https://doi.org/10.1063/1.4851955

Binder-free Ge-three dimensional graphene electrodes for high-rate capacity Li-ion batteries

Cite as: Appl. Phys. Lett. **103**, 253903 (2013); https://doi.org/10.1063/1.4851955
Submitted: 09 September 2013 • Accepted: 01 December 2013 • Published Online: 19 December 2013

C. D. Wang, Y. S. Chui, Y. Li, et al.

Binder-free Ge-three dimensional graphene electrodes for high-rate capacity Li-ion batteries

C. D. Wang,[1] Y. S. Chui,[1] Y. Li,[1,2] X. F. Chen,[1,a)] and W. J. Zhang[1,a)]
[1]*Center of Super-Diamond and Advanced Films (COSDAF) and Department of Physics and Materials Science, City University of Hong Kong, Hong Kong, China*
[2]*Department of Polymer Science and Engineering, Soochow University, Suzhou 215123, China*

(Received 9 September 2013; accepted 1 December 2013; published online 19 December 2013)

A binder-free, high-rate Ge-three dimensional (3D) graphene composite was synthesized by directly depositing Ge film atop 3D graphene grown by microwave plasma chemical vapor deposition on Ni substrate. The Ge-3D graphene structure demonstrates excellent electrochemical performance as a lithium ion battery (LIB) anode with a reversible capacity of 1140 mAh g^{-1} at 1/3C over 100 cycles and 835 mAh g^{-1} at 8C after 60 cycles, and significantly a discharge capacity of 186 mAh g^{-1} was still achieved at 32C. The high capacity and outstanding stability of the Ge-3D graphene composite propose it as a promising electrode in high-performance thin film LIBs.
 [http://dx.doi.org/10.1063/1.4851955]

Rechargeable lithium ion batteries (LIBs) have been considered as one of the most suitable candidates in relieving energy demands because of its environmental benignity, low-cost, long-life, renewability and high capacity.[1,2] Thus far, LIBs have been widely utilized in portable electronics (e.g., mobile phones and laptops), hybrid electronic vehicles, storage of renewable energy, and so forth.[3–5] Current commercial graphite anode delivers a theoretical specific capacity of 372 mAh g^{-1} due to the low gravimetric energy density of carbonaceous materials to form LiC_6 intercalated compound ($Li + 6C \leftrightarrow LiC_6$).[6] To improve cell performance, LIBs with high energy density and long cycle life are required. For this purpose, Si and Ge, the other two group IV elements as carbon, have emerged as potential candidates for high capacity anode materials because their theoretical capacities reach 4200 and 1600 mAh g^{-1}, respectively.[7–9]

Although Ge is analogous to Si, the study on its LIB applications lags greatly behind that of Si because of its high cost and relatively low capacity. Nevertheless, Ge has its own advantages in high-power LIB application because of its higher carrier mobilities, i.e., the electrical conductivity and Li diffusion coefficient are 10^4 and 4×10^2 times, respectively, higher than those of Si at room temperature.[10–13] Moreover, Ge experiences much less native oxide layer on its surface compared with Si.[14,15] Despite of these superior properties, however, an electrode based on pure Ge exhibits poor performance because of its dramatic capacity decay caused by large volume change during the lithiation and delithiation processes.[16,17] Several approaches have been proposed to buffer the volume change, such as carbon nanotube (CNT)/Ge nanoparticles core/shell structure,[18] Cu nanowire/Ge nanoparticles,[19] Ge nanowire/graphene,[20,21] Ge nanoparticle/graphene (carbon),[14,22–24] Si/Ge bilayer nanotubes,[25] nanostructured Ge films,[26] and Ge nanoparticles-reduced graphene oxide (RGO) composites.[27–29] Among them, it was found that compositing Ge with a carbon shell can effectively moderate its kinetic properties toward electron and Li ion transport, and the carbon shell also acts as a cushion in alleviating the internal stress induced upon volume change, preventing cracking, pulverization, and aggregation of Ge electrode.[15]

Graphene, a planar monolayer sheet of sp^2-hybridized carbons arranged in a two-dimensional hexagonal lattice, has the highest reported electron mobilities (200 000 cm^2/vs),[30] extremely good thermal conductivity (~3080 W/mK), and excellent flexibility.[31] The outstanding thermal, electronic, and mechanical properties make graphene an ideal candidates for application as a matrix to host nanostructured Ge to accommodate the large volume changes during the Li uptake and release processes, offer efficient electric conducting channels, and alleviate the pulverization and aggregation of Ge. Combining Ge nanostructures with graphene is a promising approach to improve the electrochemical performance of Ge-based anodes in LIBs. In this work, we report the synthesis of Ge-3-dimensional (3D) graphene composite structure and demonstrate its improved cycling and high-rate capacity as a LIB anode.

3D graphene was grown on a 25 μm thick nickel foil (Alfa Aesar No: 12722) of ~1.4 cm in diameter by using microwave plasma chemical vapor deposition (MPCVD).[32,33] After growth for 20 min, the plasma was switched off, and the sample was cooled down naturally. Ge film was subsequently deposited onto the 3D graphene scaffold by thermal evaporation in a different deposition chamber with a base pressure of 4×10^{-7} mbar. The thickness of Ge film was monitored by a 1300 MHz counter-timer (black-star). Other details about the growth and characterization of 3D graphene and Ge film, and electrochemical measurements, were given in Ref. 34.

The morphology of the as-grown 3D graphene was studied by scanning electron microscopy (SEM), as shown in Fig. 1(a). It can be found that the synthesized graphene is in a 3D foothill-like structure, different from the traditional 2-dimensional (2D) flat graphene sheets grown atop Cu foils.[35] Similar 3D graphene pedals were previously reported to grow on graphite fibers and silicon substrate under hydrogen MPCVD, and the formation of energetic growth in the presence of plasmas is suggested to be responsible for the 3D

a)Authors to whom correspondence should be addressed. Electronic addresses: xianfeng.chen@cityu.edu.hk and apwjzh@cityu.edu.hk.

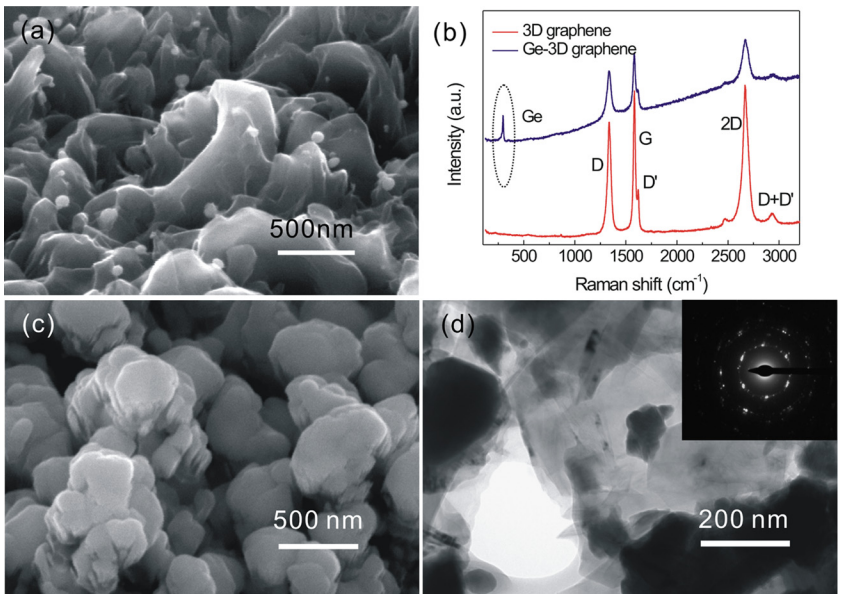

FIG. 1. (a) SEM image of 3D graphene scaffold obtained at a tilted angle of 45°, (b) Raman spectrum of the 3D graphene scaffold, (c) SEM image of Ge-3D graphene composite obtained at a tilted angle of 45°, (d) TEM image of Ge-3D graphene composite, the inset is the corresponding SAED pattern measured on the center Ge nanoparticle.

graphene growth.[36–38] Visible Raman spectrum obtained with laser wavelength of 633 nm reveals an intensive G and 2D (G′) peak of the as-grown graphene accompanying with a relative strong D peak as shown in Fig. 1(b), which verifies the formation of multilayer graphene and suggests that the obtained 3D graphene is more defective compared with the typical 2D graphene.[35] After Ge deposition, the intensities of D, G, and 2D peaks decrease concurrently due to the coverage of Ge film. However, the intensity ratio of the D to G peaks maintains almost the same, implying that defects were not increased noticeably during Ge deposition. As highlighted by the dotted circle, a new peak centered at 300 cm^{-1} appears, which is assigned to the Raman LO mode of Ge.[39] No characteristic peak for germanium oxide could be observed. Fig. 1(c) shows the SEM morphology of Ge film deposited by thermal evaporation atop the 3D graphene scaffold. The Ge film completely covers the surface of the 3D graphene and presents a mushroom-structure. Note that the Ge-3D graphene composite structure was directly used as electrode without adding any binder in the half-cell test as discussed below. The elimination of the non-conducting polymeric binders in the anode is beneficial to improving the storage capacity to some extent and makes the process adaptable to the construction of nanostructured thin film LIBs.

Transmission electron microscopy (TEM) was carried out to study the structure of Ge-3D graphene electrode, as shown in Fig. 1(d). It can be seen that the graphene sheet is transparent and flexible. The graphene sheet has a multilayer structure, as confirmed by TEM studies reported in our recent work.[33] Ge nanoparticles were found to decorate on graphene. The uneven distribution of the Ge nanoparticles was considered to be due to the sonication during the TEM sample preparation, by which part of the Ge layer was delaminated and peeled off from the graphene surface. The insert of Fig. 1(d) shows the selected area electron diffraction (SAED) pattern of the nanoparticle at the center of Fig. 1(d), which further identifies the polycrystalline nature of the Ge layer.

To verify the superiority of the binder-free Ge-3D graphene as a high-rate anode material for LIBs, electrochemical measurements were carried out. As 3D graphene also participates in the electrochemical reactions, we consider 3D graphene with Ge thin film as a composite. The mass of carbon (including 3D graphene and the dissolved carbon in Ni foil) is about 0.11 mg, and the mass of Ge is about 0.36 mg, corresponding to areal mass loadings of about 7.15 mg/cm^2 for carbon and 23.40 mg/cm^2 for Ge. If we assume all dissolved carbon atoms in Ni foil diffuse back to its surface and form graphene, the theoretical capacity (1C) of the Ge-3D graphene composite should be 1312 mAh g^{-1}. More discussions about these have been given in our previous works in detail. As discussed previously,[33] the calculated specific capacity of Ge-3D graphene presented in this work could be underestimated by up to 8.5%. Fig. 2(a) shows the 1st, 2nd, 3rd galvanostatic

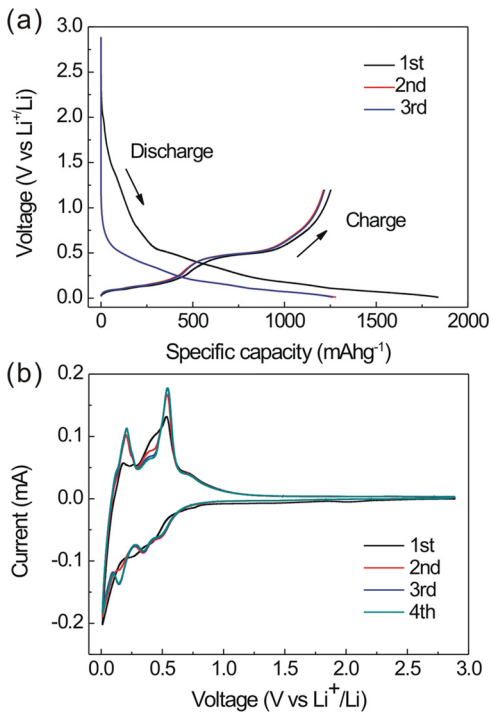

FIG. 2. (a) Charge-discharge profiles of 1st, 2nd, 3rd cycles for Ge-3D graphene at 1/3C, (b) CVs of Ge-3D graphene for the first to the fourth cycle at a scan rate of 0.1 mV/s, and a potential range of 0–2.9 V vs. Li^+/Li.

charge-discharge profiles of Ge-3D graphene electrode under a current density of 1/3C (1C = 1312 mAh g^{-1}) over a voltage range of 0–1.25 V vs Li^+/Li. The initial discharge and charge specific capacity are 1840 and 1281 mAh g^{-1}, respectively, which are significant larger than the theoretical capacity value of the composite. The excess capacity could be attributed to the formation of solid-electrolyte interface (SEI) layers on the surface of electrode due to electrolyte decomposition.[40] Meanwhile, the Coulombic efficiency (the ratio between charge and discharge) was 68% for the first cycle and dramatically increased to 94% in the subsequent cycles. The curves for the second and the third cycles in fact overlap, which suggests that the cycling quickly stabilizes without palpably decaying during further Li^+ uptake and release processes.

To further understand the electrochemical reaction behaviors of Li^+ during uptake and release processes, cyclic voltammogram (CV) measurements were performed over the range of 0.0–2.9 V vs. Li^+/Li at a scan rate of 0.1 mV/s for four cycles (Fig. 2(b)). In the first cycle, a broad cathodic peak at about 0.25 V was revealed. It is in consistent with the observation of the stable plateau in the first discharge curve in Fig. 2(a), which should be assigned to the multistep electrochemical reduction reactions of Ge with Li to form Li_xGe alloys. In the second to fourth cycles, three cathodic peaks at 0.14, 0.34, and 0.5 V are assigned to different lithium intercalation processes. Upon anodic scan, the peaks located at 0.53 V can be attributed to the oxidation of Li_xGe to Ge. Furthermore, discernible reduction and oxidation peaks at 0.1–0.25 V are also presented, which comes from the insertion/extraction of Li into/from graphene matrixes.[41] Note that after the first cycle, the 2nd–4th cycling curves largely overlap with each other. It is in consistent with the observations in charge-discharge profiles in Fig. 2(a), which reveals the electrochemical reactions quickly stabilized.

Fig. 3(a) shows the cycling performance of Ge-3D graphene under 1/3C rate (437 mAh g^{-1}). It was tested galvanostatically at a low current density of C/10 for the first cycle while at C/5 for the next two cycles and at C/3 for the rest cycles. An outstanding cycling stability is revealed in Fig. 3(a). A reversible capacity as high as 1140 mAh g^{-1} after 100 cycles with about 95% retention compared with the 4th cycle (the first cycle under 1/3C rate) is achieved. The excellent cycling stability can possibly be attributed to the adoption of flexible 3D graphene scaffold which can effectively buffer the volume changes during Li^+ uptake and release process. For comparison, Ge is also directly deposited atop a Ni substrate by thermal evaporation under the same preparation conditions. The cycling performance of Ge-Ni under 1/3C rate is demonstrated in Fig. 3(a). Different from cycling behavior of Ge-3D graphene, the capacity decreases steadily and keeps a retention capacity of 188 mAh g^{-1} in the 100th cycle. In addition, the Coulombic efficiency of Ge-3D graphene under 1/3C rate is 94% in the second cycle and 97% in the following cycles. The high efficiency should be assigned to the fact that the 3D graphene enlarges the contact area between graphene and Ge electrode which can shorten the diffusion distance for lithium and electrons transport between the electrolyte and the current collector. The high conductivity of graphene also enables high speed transportation for lithium and electrons. The rate

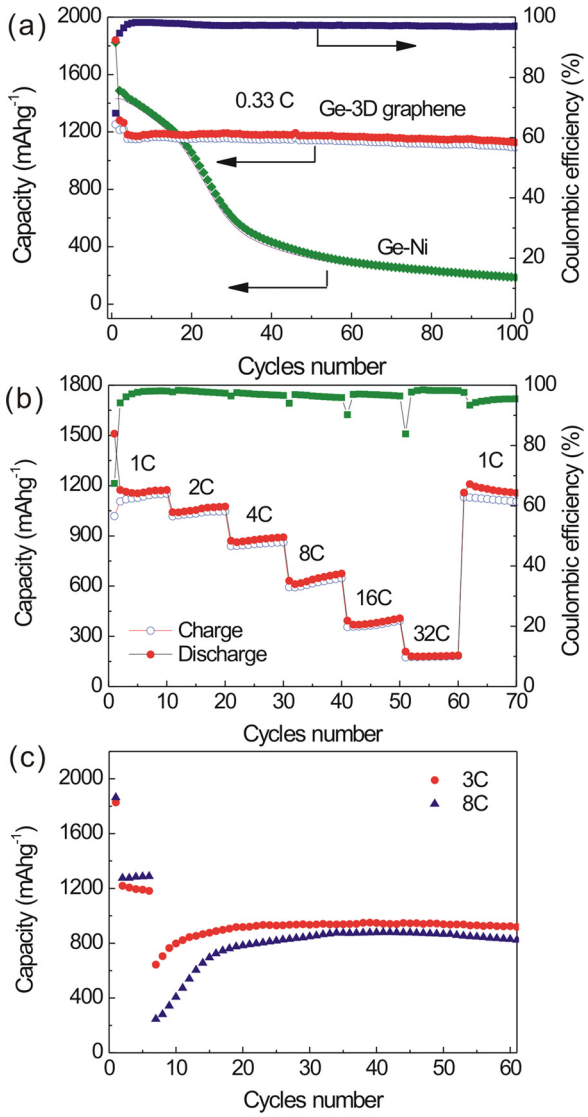

FIG. 3. (a) Cycling performance of Ge-3D graphene and Ge-Ni electrodes under 1/3C rate, (b) galvanostatic charge/discharge capacities at various rates from 1C to 32C, (c) charge/discharge capacities versus cycling number for Ge-3D graphene at the rate of 3C and 8C, respectively.

capacity performances are demonstrated in Fig. 3(b). The results show that the Ge-3D graphene electrode delivers discharge capacities of 1174, 1074, 891, 675, and 408 mAh g^{-1} at 1C, 2C, 4C, 8C, and 16C, respectively. Particularly a discharge capacity of 186 mAh g^{-1} was still achieved at a very high current density of 32C. In addition, it is found that a stable specific capacity of 1131 mAh g^{-1} (98.5% of the initial capacity at 1C rate) could be recovered once the current density was reduced back to the initial 1C after sixty cycles with increased current density up to 32C. The Coulombic efficiencies at different rates (Fig. 3(b)) were mostly higher than 96% except at several turning points between different rates. The superior rate capacity performances suggest that Ge-3D graphene may be a promising anode material in high-performance thin film LIBs where fast charge/discharge rates are desirable. To further identify the high rate cycling performances of Ge-3D graphene, the electrode was also tested under 3C and 8C. From the results shown in Fig. 3(c), it can be seen that capacities of 931 and 835 mAh g^{-1} can be obtained after 60 cycles. During the cycling, the capacity

first decreases and then increases. Similar trends of capacity were also observed by Guo *et al.*[42] and in our previous work[33] in Si-based electrodes which were considered to be due to the gradual activation of Si in the charging/discharging processes.

Various Ge-carbon composite structures for anode application in LIBs have been reported recently; the incorporation of graphene has been illustrated to be a promising approach to improve the anode performance, as summarized in Table S1 of supplementary material.[34] Among the anodes comprising carbon and Ge nanostructures, Ge nanowire/graphene[20] and CNT/Ge nanoparticles[18] core-shell nanostructures demonstrated much better overall performance, and our Ge nanoparticles-3D graphene anode depicted a comparable or even superior specific capacity and cycling performance to other Ge-carbon structures as listed in Table SI of the supplementary material.[34] In particular, if we compare our anode with the closely relevant ones composed of Ge nanoparticles and RGO,[27–29] the 3D graphene employed in this work appeared to further improve the performance. The higher crystallinity and conductivity of the 3D graphene with respect to RGO facilitated electron and Li ion transfer, and 3D graphene could also accommodate large volume change during cycling processes.[33] Moreover, the Ge-3D graphene anodes were prepared using thin film technology, which may benefit the fabrication of all-solid-state thin film LIBs.

In conclusion, we have developed a two-step route for preparing Ge-3D graphene electrodes by MPCVD and thermal evaporation. As an anode material for Li-ion batteries, the Ge-3D graphene composite electrodes exhibit excellent cycling performance which delivers a reversible capacity of 1140 mAh g^{-1} (95% retention compared with the initial one) up to 100 cycles. It also demonstrates excellent high-rate capacities of 931 and 835 mAh g^{-1} after 60 cycles at current densities of 3C and 8C, respectively. These outstanding performances may be ascribed to the electronically conductivity, macroporousness, and flexibility of 3D graphene, which could provide superior conduction path for electrons and ions transportation and accommodate the volume changes upon Li^+ uptake and release processes.

This work was supported by National Natural Science Foundation of China (NSFC Grant No. 61176007) and Research Grants Council of the Hong Kong Special Administrative Region, China (Project No. CityU 102010).

[1]Z. H. Wen, Q. Wang, Q. Zhang, and J. H. Li, Adv. Funct. Mater. **17**, 2772 (2007).
[2]M. S. Whittingham, Chem. Rev. **104**, 4271 (2004).
[3]B. Wang, J. S. Chen, H. B. Wu, Z. Wang, and X. W. Lou, J. Am. Chem. Soc. **133**, 17146 (2011).
[4]M. Armand and J. M. Tarascon, Nature **451**, 652 (2008).
[5]H. Li, Z. X. Wang, L. Q. Chen, and X. J. Huang, Adv. Mater. **21**, 4593 (2009).
[6]B. J. Landi, M. J. Ganter, C. D. Cress, R. A. DiLeo, and R. P. Raffaelle, Energy Environ. Sci. **2**, 638 (2009).
[7]M. Winter, J. O. Besenhard, M. E. Spahr, and P. Novák, Adv. Mater. **10**, 725 (1998).
[8]M. Park, K. Kim, J. Kim, and J. Cho, Adv. Mater. **22**, 415 (2010).
[9]C. Chan, H. L. Peng, G. Liu, K. McIlwrath, X. F. Zhang, R. A. Huggins, and Y. Cui, Nat. Nanotechnol. **3**, 31 (2008).
[10]L. P. Tan, Z. Lu, H. T. Tan, J. Zhu, X. Rui, Q. Yan, and H. H. Hng, J. Power Sources **206**, 253 (2012).
[11]J. Graetz, C. C. Ahn, R. Yazami, and B. Fultz, J. Electrochem. Soc. **151**, A698 (2004).
[12]D. Wang, Y.-L. Chang, Q. Wang, J. Cao, D. B. Farmer, R. G. Gordon, and H. J. Dai, J. Am. Chem. Soc. **126**, 11602 (2004).
[13]C. S. Fuller and J. C. Severiens, Phys. Rev. **96**, 21 (1954).
[14]D. J. Xue, S. Xin, Y. Yan, K. C. Jiang, Y. X. Yin, Y. G. Guo, and L. J. Wan, J. Am. Chem. Soc. **134**, 2512 (2012).
[15]H. Seo, M. H. Park, K. T. Lee, K. T. Kim, J. Y. Kim, and J. P. Cho, Energy Environ. Sci. **4**, 425 (2011).
[16]G. Cui, L. Gu, L. Zhi, N. Kaskhedikar, P. A. V. Aken, and K. Mullen, Adv. Mater. **20**, 3079 (2008).
[17]C. M. Park, J. H. Kim, H. S. Kim, and H. J. Sohn, Chem. Soc. Rev. **39**, 3115 (2010).
[18]I. S. Hwang, J. C. Kim, S. D. Seo, S. Lee, J. H. Lee, and D. W. Kim, Chem. Commun. **48**, 7061 (2012).
[19]J. Wang, N. Du, H. Zhang, J. Yu, and D. Yang, J. Mater. Chem. **22**, 1511 (2012).
[20]H. Kim, Y. Son, C. Park, J. Cho, and H. C. Cho, Angew. Chem., Int. Ed. **52**, 5997 (2013).
[21]C. Wang, J. Ju, Y. Yang, Y. Tang, J. Lin, Z. Shi, R. P. S. Han, and F. Huang, J. Mater. Chem. A **1**, 8897 (2013).
[22]H. Lee, H. Kim, S. G. Doo, and J. Cho, J. Electrochem. Soc. **154**, A343 (2007).
[23]C. H. Kim, H. S. Im, Y. J. Cho, C. S. Jung, D. M. Jang, Y. Myung, H. S. Kim, S. H. Back, Y. R. Lim, C. W. Lee, J. Park, M. S. Song, and W. I. Cho, J. Phys. Chem. C **116**, 26190 (2012).
[24]G. Jo, I. Choi, H. Ahn, and M. J. Park, Chem. Commun. **48**, 3987 (2012).
[25]T. Song, H. Cheng, H. Choi, J. H. Lee, H. Han, D. H. Lee, D. S. Yoo, M. S. Kwon, J. M. Choi, S. G. Doo, H. Chang, J. Xiao, Y. Huang, W. I. Park, Y. C. Chung, H. Kim, J. A. Rogers, and U. Paik, ACS Nano **6**, 303 (2012).
[26]N. G. Rudawski, B. L. Darby, B. R. Yates, K. S. Jones, R. G. Elliman, and A. A. Volinsky, Appl. Phys. Lett. **100**, 083111 (2012).
[27]J. Cheng and J. Du, Cryst. Eng. Comm. **14**, 397 (2012).
[28]C. Zhong, J. Z. Wang, X. W. Gao, D. Wexler, and H. K. Liu, J. Mater. Chem. A **1**, 10798 (2013).
[29]J. G. Ren, Q. H. Wu, H. Tang, G. Hong, W. J. Zhang, and S. T. Lee, J. Mater. Chem. A **1**, 1821 (2013).
[30]S. V. Morozov, K. S. Novoselov, M. I. Katsnelson, F. Schedin, D. C. Elias, J. A. Jaszczak, and A. K. Geim, Phys. Rev. Lett. **100**, 016602 (2008).
[31]A. A. Balandin, S. Gjpsj, W. Bao, I. Calizo, D. Teweldebrhan, F. Miao, and N. Chun, Nano Lett. **8**, 902 (2008).
[32]C. D. Wang, Y. Li, Y. S. Chui, Q. H. Wu, X. F. Chen, and W. J. Zhang, Nanoscale **5**, 10599 (2013).
[33]C. D. Wang, Y. S. Chui, R. G. Ma, T. L. Wong, J. G. Ren, Q. H. Wu, X. F. Chen, and W. J. Zhang, J. Mater. Chem. A **1**, 10092 (2013).
[34]See supplementary material at http://dx.doi.org/10.1063/1.4851955 for the growth and characterization of 3D graphene and Ge film, electrochemical measurements, and Table S1 for cycling performance of the selected Ge-carbon based anodes in LIBs.
[35]C. D. Wang, Y. G. Zhou, L. F. He, T. W. Ng, G. Hong, Q. H. Wu, F. Gao, C. S. Lee, and W. J. Zhang, Nanoscale **5**, 600 (2013).
[36]Y. S. Jung, K. T. Lee, J. H. Ryu, D. Im, and S. M. Oh, J. Electrochem. Soc. **152**, A1452 (2005).
[37]W. M. Zhang, J. S. Hu, Y. G. Guo, S. F. Zheng, L. S. Zhong, W. G. Song, and L. J. Wan, Adv. Mater. **20**, 1160 (2008).
[38]A. Malesevic, R. Vitchev, K. Schouteden, A. Volodin, L. Zhang, G. V. Tendeloo, A. Vanhulsel, and C. V. Haesendonck, Nanotechnology **19**, 305604 (2008).
[39]T. R. Yang, M. M. Dvoynenko, Z. C. Feng, and H. H. Cheng, Eur. Phys. J. B **31**, 41 (2003).
[40]P. G. Bruce, B. Scrosati, and J. M. Tarascon, Angew. Chem., Int. Ed. **47**, 2930 (2008).
[41]L. Y. Beaulieu, K. C. Hewitt, R. L. Turner, A. Bonakdarpour, A. A. Abdo, L. Christensen, K. W. Eberman, L. J. Krause, and J. R. Dahn, J. Electrochem. Soc. **150**, A149 (2003).
[42]F. F. Cao, J. W. Deng, S. Xin, H. X. Ji, O. G. Schmidt, L. J. Wan, and Y. G. Guo, Adv. Mater. **23**, 4415 (2011).